

# Preparation of High Percentage $\alpha$ -Calcium Sulfate Hemihydrate via a Hydrothermal Method

Le Fu<sup>1</sup>, Wei Xia<sup>1</sup>, Torbjörn Mellgren<sup>1</sup>, Mikael Moge<sup>2</sup>, Håkan Engqvist<sup>1\*</sup>

<sup>1</sup>Applied Materials Science, Department of Engineering Sciences, Uppsala University, Uppsala, Sweden

<sup>2</sup>BioArctic Neuroscience AB, Stockholm, Sweden

Email: \*hakan.engqvist@angstrom.uu.se

**How to cite this paper:** Fu, L., Xia, W., Mellgren, T., Moge, M. and Engqvist, H. (2017) Preparation of High Percentage  $\alpha$ -Calcium Sulfate Hemihydrate via a Hydrothermal Method. *Journal of Biomaterials and Nanobiotechnology*, 8, 36-49.  
<http://dx.doi.org/10.4236/jbnb.2017.81003>

**Received:** October 12, 2016

**Accepted:** January 1, 2017

**Published:** January 4, 2017

Copyright © 2017 by authors and Scientific Research Publishing Inc. This work is licensed under the Creative Commons Attribution International License (CC BY 4.0).

<http://creativecommons.org/licenses/by/4.0/>



Open Access

## Abstract

$\alpha$ -calcium sulfate hemihydrate ( $\alpha$ -HH) is known to be suitable for application as bone void filler. High percentage of  $\alpha$ -HH is obviously needed for medical applications, especially for implantation. Three commercially available calcium sulfate dihydrates (DH,  $\text{CaSO}_4 \cdot 2\text{H}_2\text{O}$ ) with different sizes and surface morphologies were used as starting materials to synthesize high percentage  $\alpha$ -HH via a hydrothermal method. The median particle sizes of the three types of DH were 946.7  $\mu\text{m}$ , 162.4  $\mu\text{m}$  and 62.4  $\mu\text{m}$ , respectively. They were named as DH-L, DH-M and DH-S in this paper. The particle size distribution, morphology and phase composition of the raw materials were evaluated before synthesis. SEM results revealed that DH-L consisted of irregular large particles, while DH-M and DH-S were composed of plate-like particles with some small ones. High percentage HH can be obtained with proper synthesis parameters by hydrothermal method, specifically, 105°C/90 min for DH-L (achieving 98.8% HH), 105°C/30 min for DH-M (achieving 96.7% HH) and 100°C/45 min for DH-S (achieving 98.4% HH). All the synthesized HH were hexagonal columns, demonstrating that they were  $\alpha$ -phase HH. The particle size and morphology of starting material (DH) have significant influences on not only the rate of phase transition but also the morphology of the synthesized  $\alpha$ -HH. Calcium sulfate dihydrate cements were prepared by the synthesized  $\alpha$ -HH. The highest compressive strength of calcium sulfate dihydrate cement was 17.2 MPa. The results show that the preparation of high percentage  $\alpha$ -HH is feasible via a hydrothermal method and the process can be further scaled up to industrial scale production.

## Keywords

$\alpha$ -Calcium Sulfate Hemihydrate, High Percentage, Hydrothermal Method, Calcium Sulfate Dihydrate Cement

## 1. Introduction

Flue gas desulfurization (FGD) gypsum, mainly composed of calcium sulfate dihydrate

(DH,  $\text{CaSO}_4 \cdot 2\text{H}_2\text{O}$ ), is a byproduct produced in large amount during the desulfurization process. Nowadays, the management and utilization of FGD gypsum have become a significant issue [1]. Preparation of calcium sulfate hemihydrate (HH,  $\text{CaSO}_4 \cdot 0.5\text{H}_2\text{O}$ ) utilizing DH as raw material is one of the most promising alternatives to recycle DH and also manufacture HH which is a very useful material especially in the building industry [2] [3] [4]. There are two types of HH:  $\alpha$ -form and  $\beta$ -form. They present great differences in term of structure and property. Extensive studies have shown that  $\alpha$ -HH consists of characteristic hexagonal columnar crystalline grain with obvious and sharp crystal edges, whereas  $\beta$ -HH is composed of irregular and flaky crystals [5] [6].  $\alpha$ -HH is a metastable phase. It can be not only hydrated to become DH but also dehydrated to become calcium sulfate anhydrite (AH,  $\text{CaSO}_4$ ). The metastable life time (MLT) period, in which a metastable phase maintains its form, of  $\alpha$ -HH is affected by some factors, such as temperature, liquid medium, etc. [3] [7]. Due to  $\alpha$ -HH's better paste workability and higher mechanical strength of the hardened material, it exhibits a notably advantageous performance over  $\beta$ -HH in a wide range of fields, such as modern construction industry, molding, binder system, orthopedic and other medical applications [2] [6].

Calcium sulfate has been used to treat bone defects since the 19th century. Advantages of calcium sulfate are its osteoconductive properties and rapid resorption with minimal inflammatory response [8] [9]. For medical application, high purity is definitely significant. Medical grade  $\alpha$ -calcium sulfate hemihydrate cylindrical pellet is commercially available now, for instance, OsteoSets<sup>®</sup> from Wright Medical Arlington (USA). And also, patents have reported methods of producing surgical grade calcium sulfate by dehydrating-rehydrating and precipitation [10] [11] [12].

Commercial production of  $\alpha$ -HH involves converting FGD gypsum to  $\alpha$ -HH at elevated temperature (100°C - 150°C) under elevated pressure (138 - 414 KPa) in an atmosphere of saturated vapor in an autoclave, which is known as Autoclave Method [2] [4]. It has been widely reported that  $\alpha$ -HH can also be prepared by heating FGD gypsum in various salt or acid solutions near boiling point under atmospheric pressure, which is termed as Hydrothermal Method [2] [13] [14] [15]. The hydrothermal method exhibits advantages over autoclave method in terms of purity control and energy consumption. It is more suitable for lab work because of its mild synthesis conditions. In the hydrothermal method, the formation of  $\alpha$ -HH is believed to follow dissolution-recrystallization processes. Specifically, DH dissolves into electrolytic solution to form supersaturated solution, followed by the crystallization of  $\alpha$ -HH [4] [6] [16]. Factors, such as salt or acid solutions, supersaturation, temperature, pH and impurities, exert great influences on the nucleation and crystal growth of  $\alpha$ -HH, thereby affect the morphology, crystal size and properties of the resulted products [3] [6] [17].

In the past decades, numerous investigations have been carried out on the dissolution-recrystallization process of DH and HH [15] [18] [19]. In the hydrothermal method to prepare  $\alpha$ -HH, the transformation time and temperature have been considered as very important parameters for purity control and dehydration of  $\alpha$ -HH. In present work, we optimized the reaction temperature and time to synthesize high percentage  $\alpha$ -HH by using three types of commercial DH as raw material. The effects of the morphology and particle size of the raw materials on the synthesis process were discussed.

We also investigated the strength and morphology of DH cements prepared by the synthesized  $\alpha$ -HH.

## 2. Experimental

### 2.1. Materials

Three types of commercially available calcium sulfate dihydrate (DH) with different particle sizes fabricated by three companies were used in this study as raw material for DH-HH phase transition. DH with large particle size from JRS Pharma (USA) was named as DH-L; DH with medium particle size from BK Giulini PCG (Germany) was named as DH-M; DH with small particle size from Charles B. Chrystal Co. Inc. (USA) was named as DH-S. The  $\alpha$ -HH prepared by using DH-L as raw material was nominated as  $\alpha$ -HH-L. Similarly, the other two types of  $\alpha$ -HH prepared by DH-M and DH-S were  $\alpha$ -HH-M and  $\alpha$ -HH-S, respectively. The same nomenclature principle works for DH cement prepared by  $\alpha$ -HH. For instance, Cement-L means cement prepared by the  $\alpha$ -HH-L that is synthesized by using DH-L as raw material. The nomenclature is summarized in **Table 1**.  $\beta$ -HH from Sigma (Sigma-Aldrich, St Louis, MO, USA) was also evaluated by SEM and XRD as a reference sample.

### 2.2. Methods

The experiments were performed in a 5 L double-walled cylindrical glass reactor (Globe, Syrris, UK) equipped with a glass condenser for vapor reflux, a thermometer for monitoring reaction temperature and a Teflon stirrer for homogenizing the slurry. The oil circulating through the double walls was regulated by a circulator (CF41 Cryo-Compact Circulator, Julabo, Germany) and the temperature was controlled within  $\pm 0.5^\circ\text{C}$ . In each run, 500 ml 4 mol/L calcium chloride solution was added into the reactor and preheated to expected temperature. Then, 50 g calcium sulfate dihydrate (DH) was mixed in the reactor and the slurry was kept stirring at a constant stirring rate of 270 r/min. The powder obtained by vacuum filtration was quickly rinsed with 1 L boiling water to remove residual calcium chloride, and then with 200 ml isopropanol (Sigma-Aldrich, St Louis, MO, USA) to remove water in a suction flask, followed by drying at  $60^\circ\text{C}$  for two hours.

### 2.3. Characterizations

X-ray diffraction (Diffractometer D5000, Siemens, Germany) was performed to invest-

**Table 1.** The nomenclature of the materials in this study.

Name of raw DH powder	Manufacture company	Name of $\alpha$ -HH synthesized by raw powder	Name of cement prepared by synthesized $\alpha$ -HH
DH-L	JRS Pharma, USA	$\alpha$ -HH-L	Cement-L
DH-M	BK Giulini PCG, Germany	$\alpha$ -HH-M	Cement-M
DH-S	Charles B. Chrystal Co. Inc., USA	$\alpha$ -HH-S	Cement-S

tigate the crystalline phases by using Cu K $\alpha$  X-ray at a diffraction angle from 10° to 80° with a step size of 0.02°/step and an interval of 0.2 s/step. The particle size distribution was examined on a laser diffraction particle size analyser (Mastersizer X, Malvern Instrument Ltd., UK).

SEM (TM-1000, Hitachi, Japan) was used to observe the morphology of the DH at a 500  $\times$  magnification. Higher magnification morphology observation of DH, synthesized HH and DH cements were carried out on another SEM (LEO 1550, Zeiss, Germany).

Thermal gravity analysis (Q500, TA instrument, USA) was carried out for calcium sulfate phase identification and crystal water determination. Based on the weight loss percentage recorded by Thermal gravity analysis (TGA), the content of DH, HH and AH in the synthesized powder can be determined. According to literature [5], the concentration (wt%) of crystallization water of HH is 6.2%, and that of DH is 20.9%. If the weight loss is less than 6.2% in TGA result, it means the synthesized powder is composed of HH and AH, whereas, weight loss over 6.2% indicates that the synthesized powder consists of HH and DH. In the first case, the following formula was used:  $6.2\% \times X + 0\% \times (1 - X) = Y$ , while in the latter case, the equation was  $6.2\% \times X + 20.9\% \times (1 - X) = Y$ , where X is the percentage of HH, Y is the weight loss recorded by TGA test.

The processes of making cements utilizing synthesized powders were as follows: Mix 1g of calcium sulfate powder with deionized water (about 10 - 15 s). Transfer the mixture to a syringe equipped with a 2 mm diameter tip. Inject the paste into a one side closed silicone mould with a size of 6  $\times$  13 mm, and then vibrate the sample for 15 s. Let the paste set at room temperature (21°C - 22°C) for 24 h. Remove the sample from the mould, grind it with 800<sup>#</sup> SiC grinding paper without any water and measure the compressive strength of the cement 24 hours after the cement was prepared. Compressive strength of cement was tested using an AGS-H universal material testing machine (Shimadzu, Kyoto, Japan) by applying a uniaxial compressive load at a cross-head displacement rate of 1 mm/min.

### 3. Results and Discussion

#### 3.1. Characterization of the Raw Material

Particle size distribution test demonstrated that the median particle size of DH-L was 946.7  $\mu\text{m}$  which was much larger than the other two types of DH. This is in good agreement with particle size distribution curve of DH-L which showed a sharp peak at approximately 900  $\mu\text{m}$  (Figure 1). The median particle size of DH-M and DH-S were 162.4  $\mu\text{m}$  and 62.4  $\mu\text{m}$ , respectively. There were two rough peaks of the particle size distribution of DH-M and DH-S (Figure 1). One was at 10  $\mu\text{m}$  and the other 100  $\mu\text{m}$ , indicating that these two types of DH were composed of small particles and relatively large ones. However, DH-L showed more centralized particle size distribution, concentrating upon 900  $\mu\text{m}$ . As can be seen from SEM results (Figure 2(a) & Figure 2(b)), DH-L had very large and irregular particles, which was in accordance with the result of particle size distribution test. DH-M and DH-S shared similar morphology characteristics, composing of plate-like particles. Both small and relatively large particles can be observed (Figures 2(c)-(f)). High magnification SEM images showed that DH-M pre

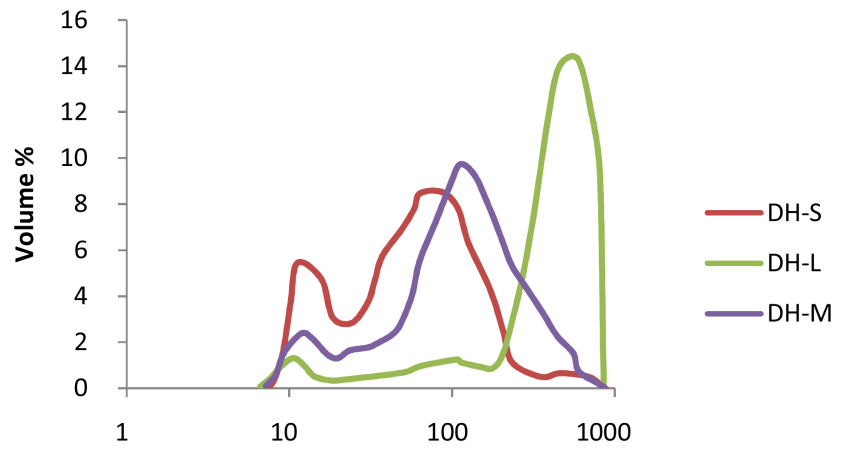


**Figure 1.** Particle size distribution of the three types of DH.

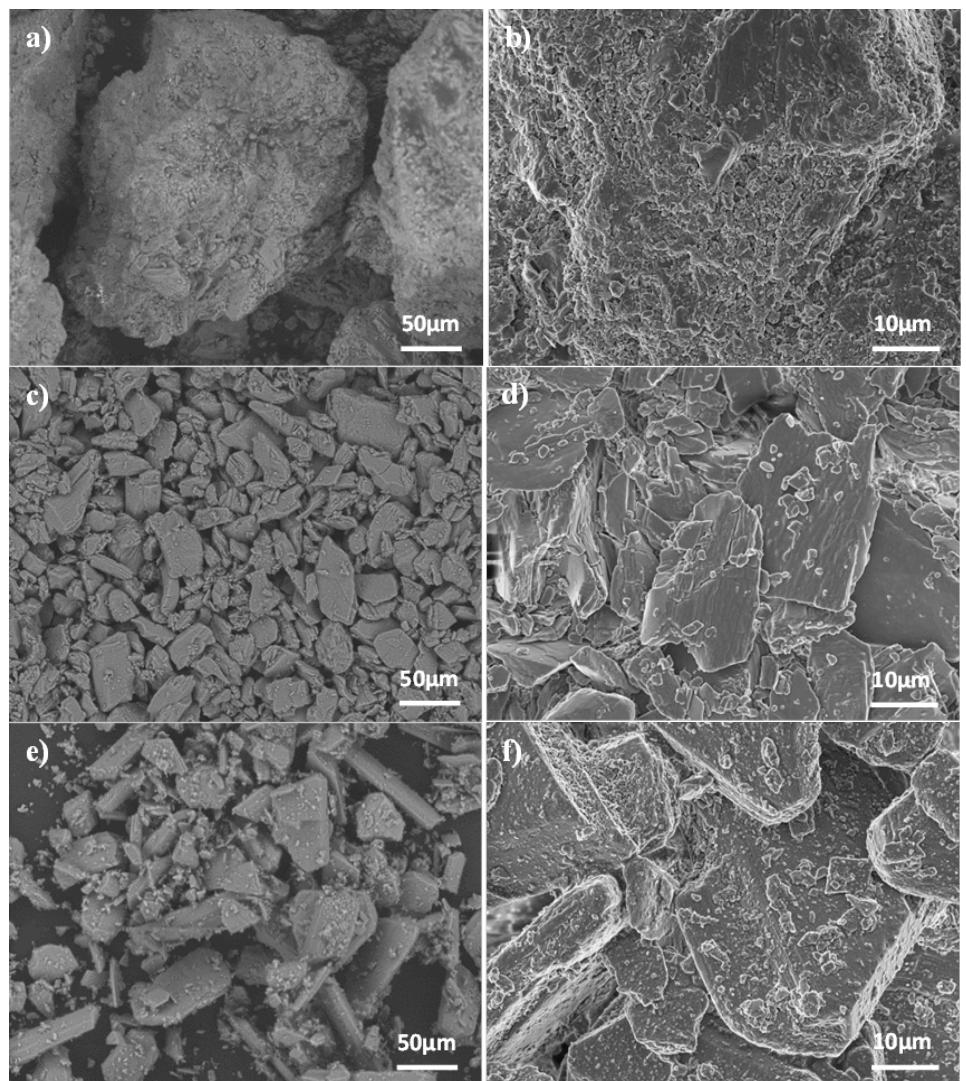


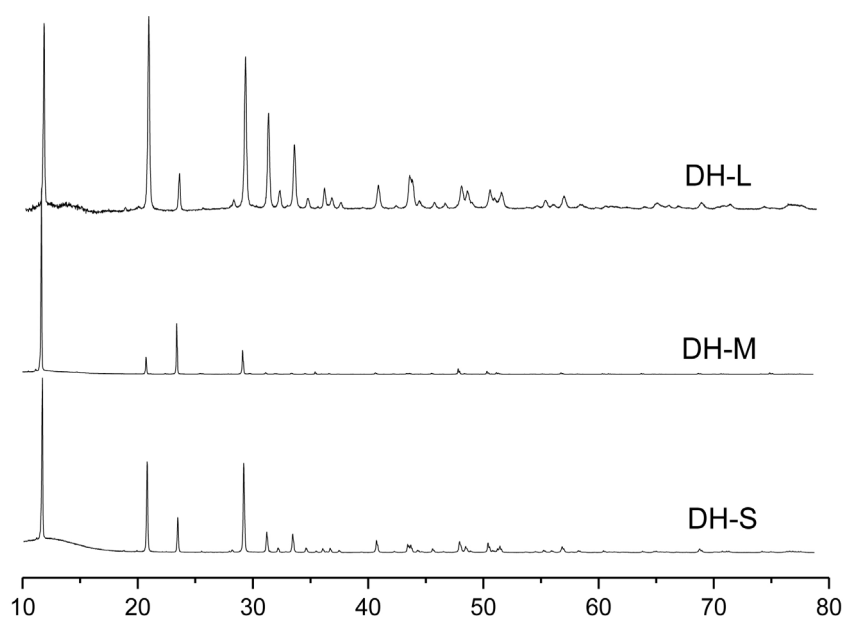
**Figure 2.** SEM images of the three types of DH: (a), (b) DH-L; (c), (d) DH-M; (e), (f) DH-S.

sented the most smooth particle surfaces (**Figure 2(d)**), while DH-S had relatively rougher particle surface with very small particles adhered on the plate-like particles

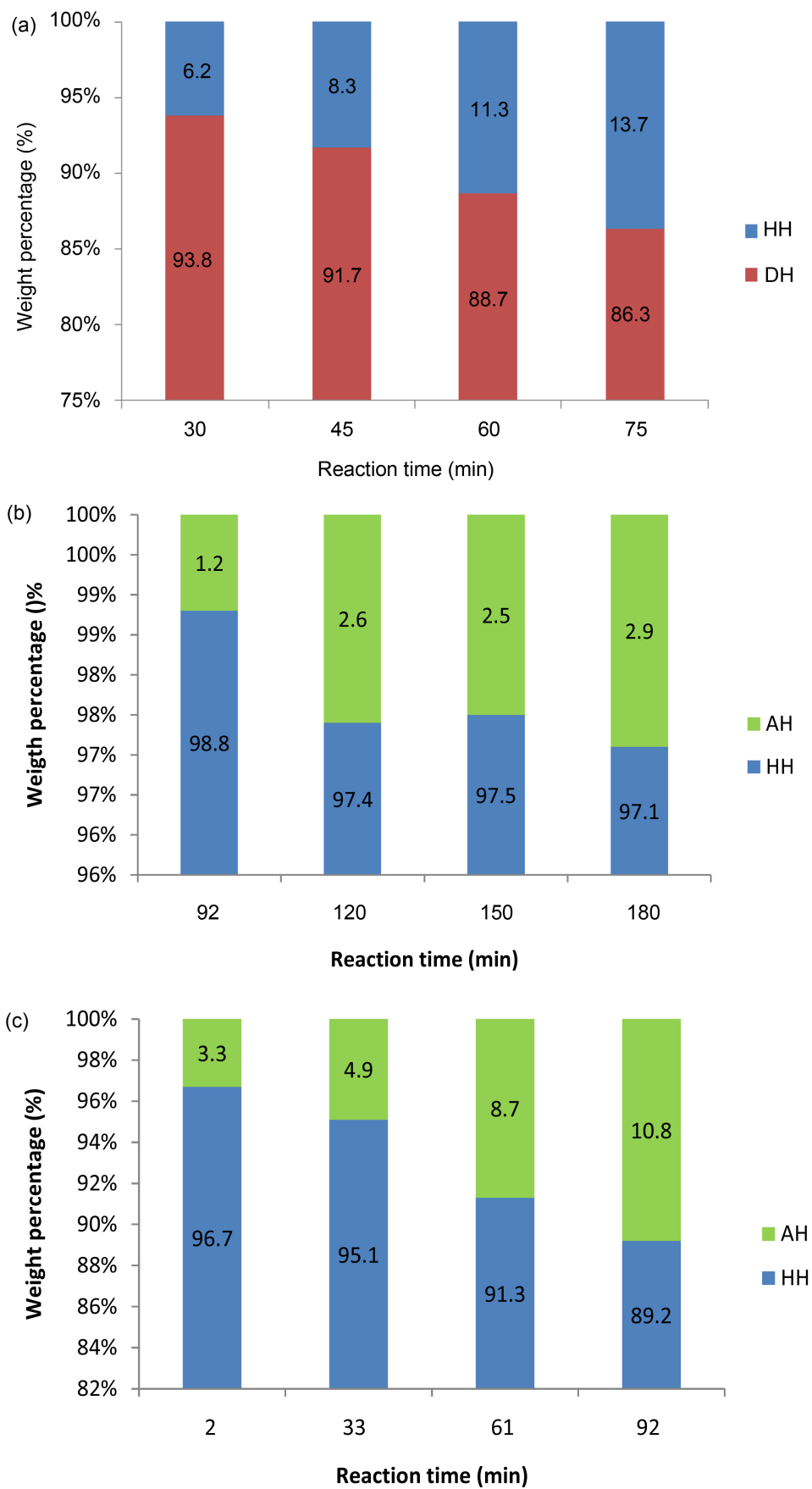
(Figure 2(f)). DH-L also presented very rough surface (Figure 2(b)). All of the raw powders showed identical XRD peak positions. Only peaks associated with the DH structure were observed. No peaks related to impurities were detected, see Figure 3. It should be noted that the peak intensities of the three types of DH were different, presumably due to preferential orientation of certain lattice planes. As mentioned before, DH-L composed of large and irregular particles, without preferential orientation, while DH-M and DH-S presented plate-like morphology which probably contains preferential orientation of certain lattice planes.

### 3.2. Synthesis of High Percentage $\alpha$ -HH

One of the major objectives of this study is to optimize the reaction time and temperature to obtain high percentage  $\alpha$ -HH. Only 13.7% DH transformed to HH within 75 min at 100°C (Figure 4(a)). Reaction temperature exerts significant influence on the rate of the transition. As can be seen from Figure 4(b), 98.8% HH can be achieved after 90 min at 105°C. For DH-M, 105°C/30 min was the proper synthesis parameters which gave 96.7% HH (Figure 4(c)). In comparison, it took much shorter time for DH-S to transform to HH, achieving as high as 98.4% HH at 100°C/45 min (Figure 4(d)). It was obvious that the reaction of DH-S and DH-M were much faster than that of DH-L. According to literatures [4] [16], the dominant mechanism of transformation between gypsum (DH) and HH in aqueous solution is believed to be a through-solution reaction. Firstly, the dissolution of DH leads to a supersaturation with respect to HH, and then the HH particles precipitate from the solution after nucleation and growth of nuclei. Therefore, the dissolution rate of DH, nucleation and growth rate of HH affects the time needed for the complete transition of DH. Both particle size distribution (Figure 1) and SEM (Figure 2(a) & Figure 2(b)) results confirmed that particle size of DH-L



**Figure 3.** XRD patterns of the raw materials. All of the observed peaks correspond to calcium sulfate dihydrate. Peak intensity differences could be due to preferential orientation.



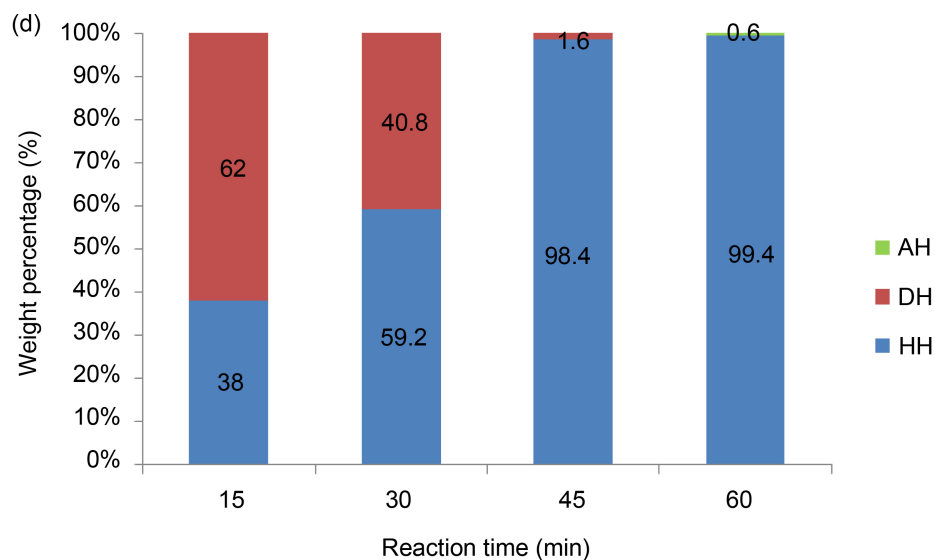


**Figure 4.** Weight percentage of HH, DH or AH after synthesis. (a) at 100°C, DH-L as raw material; (b) at 105°C, DH-L as raw material; (c) at 105°C, DH-M as raw material; (d) at 100°C, DH-S as raw material.

was much larger than the other two types of DH. Therefore, it took longer time to dissolve DH-L in the solution to form supersaturation. It was noteworthy that the synthesized powder of DH-S consisted of 98.4% HH and 1.6% DH at 100°C/45 min (**Figure 4(d)**), indicating that the transformation of DH to HH has almost finished within 45 min at 100°C which is 5°C lower than the reaction temperature of the other two types of DH. The authors would still ascribe the high transition rate of DH-S to particle size effect. The median particle size of DH-S was 62.4 μm. Hence, DH-S can dissolve into the solution to form supersaturation within shorter time. What's more, it is believed that nucleation can not only occur in the solution but also on the surface of the mother gypsum [5] [16]. As can be seen from **Figure 2(f)**, there were a large number of small particles on the surface of DH-S particles. These small particles were washed away from the surface of the seeds and they were likely to be the nucleation sites for both heterogeneous and secondary nucleation, leading to higher transition rate.

It has been widely reported that the typical morphology of  $\alpha$ -HH prepared under different conditions was a hexagon prism [3] [4] [6]. Therefore, the rod-like and prismatic particles clearly observed in **Figures 5(a)-(c)** were all  $\alpha$ -HH. In contrast, the morphology of  $\beta$ -HH was quite different, consisting of irregular and flaky particles (**Figure 5(d)**). As can be seen from **Figure 6**, XRD patterns of the three types of  $\alpha$ -HH were quite similar.  $\beta$ -HH shared great similarities in XRD patterns with  $\alpha$ -HH, except that  $\beta$ -HH presented an overlap peak at 25°, while  $\alpha$ -HH had a single peak at the same degree. SEM observation and XRD results confirm that the synthesized HH were  $\alpha$ -HH.

$\alpha$ -HH is a metastable phase, which can only maintain its form in a certain period in aqueous solution before further transit to a relatively stable phase. It is well accepted that at a given temperature solid phase that has the lowest solubility in aqueous solution is the stable phase [19] [20] [21]. Daniela *et al.* pointed that AH was the stable phase at temperatures higher than 70°C in CaSO<sub>4</sub>-based salts because of its low solubility [16].

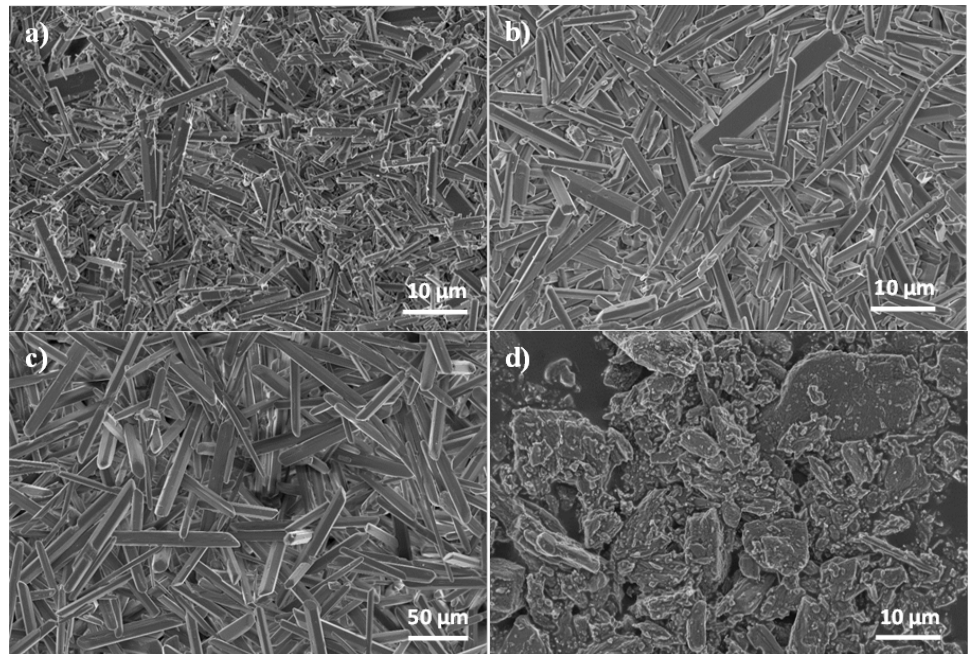


**Figure 5.** SEM micrographs of the synthesized  $\alpha$ -HH and the reference  $\beta$ -HH. (a)  $\alpha$ -HH-L-105°C/180 min; (b)  $\alpha$ -HH-M-105°C/30 min; (c)  $\alpha$ -HH-S-100°C/45 min; (d)  $\beta$ -HH.

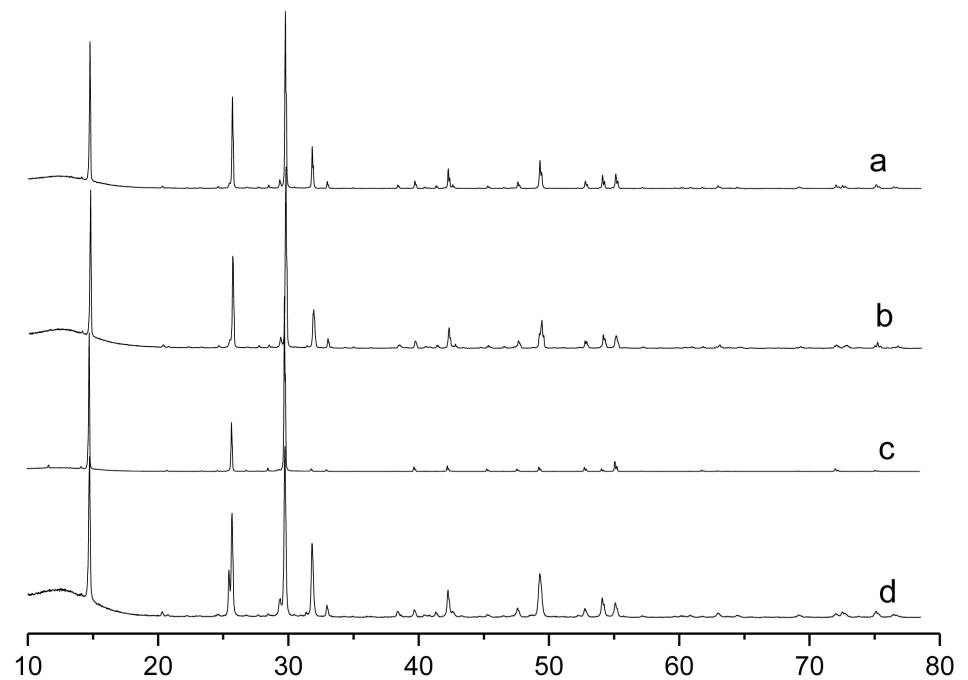


**Figure 6.** XRD patterns of  $\alpha$ -HH synthesized by different raw DH and parameters and the reference  $\beta$ -HH. Only characteristic peaks of calcium sulfate hemihydrate were detected. (a)  $\alpha$ -HH-L-105°C/180 min; (b)  $\alpha$ -HH-M-105°C/30 min; (c)  $\alpha$ -HH-S-100°C/45 min; (d)  $\beta$ -HH.

Therefore, it is understandable that AH can be detected in the synthesis experiments (**Figures 4(b)-(d)**).  $\alpha$ -HH started to transform to AH after the completion of DH-HH transformation. Moreover, with the increase of reaction time more and more  $\alpha$ -HH dehydrated to become AH. It was obvious that the dehydration rate of  $\alpha$ -HH to AH was

much slower than that of DH to  $\alpha$ -HH for the synthesis experiments, see **Figures 4(b)-(d)**. This phenomenon could be attributed to the differences on induction period of the two dehydration processes. Generally, the process of crystallization starts with a period of delay during which the solution concentration remains constant and crystal nuclei forms [21] [22]. This is so called induction period. It is influenced by several factors, such as supersaturation, temperature, component and impurities [18] [21]. Though no literature about comprehensive investigation on the induction period of crystallization processes in  $\text{CaSO}_4$ -based salts is available, based on the present results the authors tend to think that the induction period of AH crystallization is longer than that of  $\alpha$ -HH crystallization. It has been reported that the crystallization of AH is the most difficult of all calcium sulfate phase due to its slow crystallization kinetics [16].

### 3.3. The Particle Size of the Synthesized $\alpha$ -HH

Interestingly, particle size distribution test showed that the  $\alpha$ -HH-S demonstrated the largest median particle size value, 44.1  $\mu\text{m}$ . In contrast, the size of other two types of  $\alpha$ -HH was much smaller, 10.7  $\mu\text{m}$  and 3.8  $\mu\text{m}$  for  $\alpha$ -HH-M and  $\alpha$ -HH-L, respectively. **Figure 7** revealed that the particle size distribution curve of  $\alpha$ -HH-S had two peaks. One peak was at 20  $\mu\text{m}$  and the other 70  $\mu\text{m}$ , which indicated that the  $\alpha$ -HH consisted of small particles and relatively larger particles. The curves of the other two types of  $\alpha$ -HH were similar, except that  $\alpha$ -HH-L showed higher volume percentage at size of approximately 10  $\mu\text{m}$ , whereas  $\alpha$ -HH-M had higher volume percentage at around 50  $\mu\text{m}$ .  $\alpha$ -HH-M (**Figure 5(b)**) and  $\alpha$ -HH-S (**Figure 5(c)**) composed of intact and homogenous hexagon-prism-sharped  $\alpha$ -HH crystals, while  $\alpha$ -HH-L (**Figure 5(a)**) had less intact particles. The nucleation and crystal growth processes are two competitive processes in the beginning of crystallization process in terms of crystal size of the final crystallization products. Limited nuclei, low nucleation rate and high crystal growth rate results in larger crystal size, while numerous nuclei, high nucleation rate and low crystal growth rate results in smaller crystal size [6] [21] [22]. As mentioned before, the surface of the starting gypsum is able to serve as nucleation site, especially when the

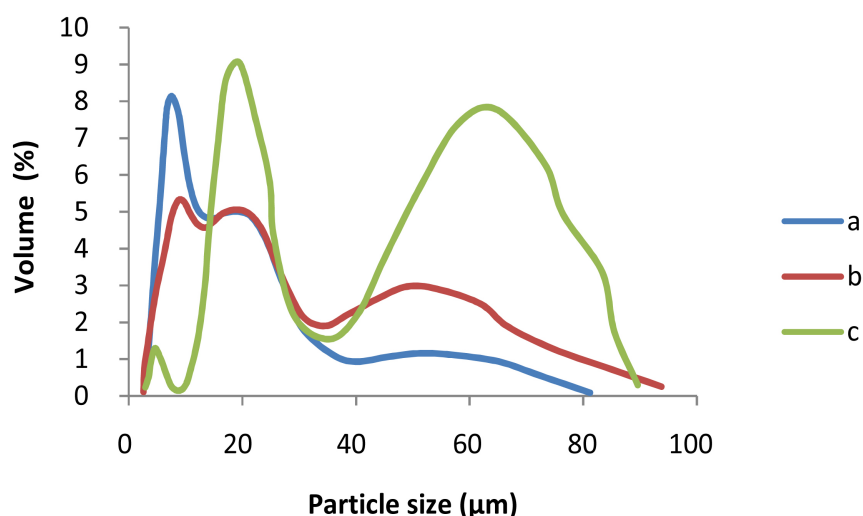


**Figure 7.** Particle size distribution of the synthesized  $\alpha$ -HH prepared by different raw DH. (a)  $\alpha$ -HH-L-105°C/180 min; (b)  $\alpha$ -HH-M-105°C/30 min; (c)  $\alpha$ -HH-S-100°C/45 min.

surface is rough. As can be seen from **Figure 2(b)**, the DH-L contained showed very rough surface which can act as sites of attachment. At the molecular level, Ca, O and S ions diffuse to the crystal surface and attach themselves to the attachment sites [21]. Numerous nucleation and growth sites in DH-L surfaces lead to the hindrance of the grain growth by impingement with neighbour grains, resulting in very small final  $\alpha$ -HH-L particles. In contrast, the surfaces of DH-M were much smoother than those of DH-L, indicating that there would be less nucleation site and nuclei compared with DH-L. Once nuclei form, Ca, O and S ions in the solution tend to crystallize on the nuclei, which result in relatively larger crystal size of the final  $\alpha$ -HH-M compared with  $\alpha$ -HH-L. Regarding the particle size of  $\alpha$ -HH-S, note that the transformation temperature of  $\alpha$ -HH-S was 100°C which is 5°C lower than those of  $\alpha$ -HH-L and  $\alpha$ -HH-M. As mentioned above, transformation temperature exerts significant influence on the synthesis results, including the percentage, morphology and particle size of synthesized  $\alpha$ -HH. Lowering transformation temperature would definitely reduce both nucleation and growth rates in the hydrothermal method by reducing the atom kinetics. Though no study has proven that temperature has more effects on nucleation rate than growth rate, the authors tend to believe that lowering temperature would exert more suppressing effects on nucleation rate than on growth rate. Hence,  $\alpha$ -HH-S particles get more chance to grow, resulting larger particle size compare to  $\alpha$ -HH-L and  $\alpha$ -HH-M.

### 3.4. DH Cements Prepared by Synthesized $\alpha$ -HH

The liquid/powder ratio and strength of DH cements prepared by synthesized  $\alpha$ -HH was shown in **Table 2**. Cement-L obtained the highest compressive strength (17.2 MPa) with a liquid/powder ratio of 0.6. In contrast, Cement-M achieved relatively lower compressive strength, 7.7 MPa, with a higher liquid/powder ratio of 0.8. These cement compressive strength values were quite close to those reported in previous literatures [23] [24].  $\alpha$ -HH-S paste can be achieved with a relatively lower liquid/powder ratio of 0.5, however, the paste was almost non-injectable. Only peaks of DH can be observed in XRD patterns (**Figure 8**), indicating that all  $\alpha$ -HH transformed to DH during cement setting. SEM observations (**Figure 9**) showed that the three types of cements were compact materials without obvious pores. They were composed of micrometre-sized plate-like crystals. No significant difference on the morphology was observed, while Cement-L showed relatively larger crystal size.

## 4. Conclusion

The synthesis parameters were optimized to obtain high percentage  $\alpha$ -HH utilizing

**Table 2.** Cement strength of the synthesized  $\alpha$ -HH (mean value  $\pm$  standard deviation).

Material	Composition	Synthesis parameters	Liquid/powder ratio	Cement strength (MPa)
Cement-L	98.8% HH	105°C/180 min	0.6	17.2 $\pm$ 1.4
Cement-M	97.2% HH	105°C/30 min	0.8	7.7 $\pm$ 1.8
Cement-S	98.4% HH	100°C/45 min	0.5	-

Note: The paste of  $\alpha$ -HH-S is non-injectable.

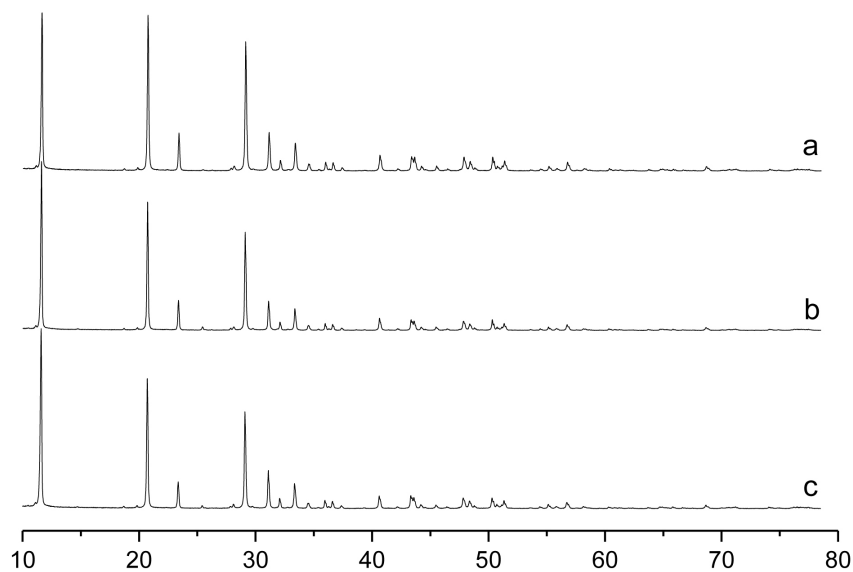


**Figure 8.** XRD patterns of the DH cements prepared by synthesized HH. All observed peaks correspond to calcium sulfate dihydrate, indicating that complete conversion to DH during cement setting. (a) Cement-L; (b) Cement-M; (c) Cement-S. Note: Cement-S sets in the syringe.

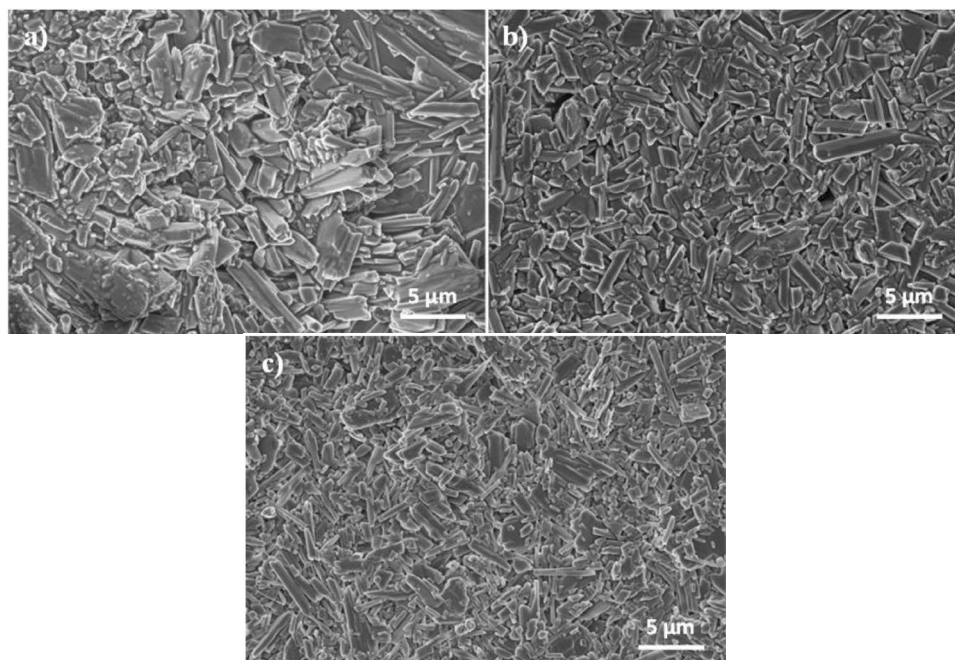


**Figure 9.** SEM micrographs of the DH cements prepared by synthesized  $\alpha$ -HH. (a) Cement-L; (b) Cement-M; (c) Cement-S. Note: Cement-S sets in the syringe.

three types of commercially available FGD gypsum with different sizes. Synthesis results showed that preparation of  $\alpha$ -HH with high percentage from calcium sulfate dihydrate with the hydrothermal method was feasible. The proper synthesis conditions were as follows: 105°C/180 min for DH-L, 105°C/30 min for DH-M, 100°C/45 min for DH-S. Particle size and morphology of DH raw material have significant influences on the synthesis result: large size DH particles with rough surfaces take longer time for the

DH-HH transformation and result in small  $\alpha$ -HH crystals, while small size DH particles with smooth surfaces show much higher transformation rate and relatively larger  $\alpha$ -HH particles. This has been ascribed to the relative rate between nucleation and growth processes. The transition rate of DH to  $\alpha$ -HH was much faster than that of  $\alpha$ -HH to AH. The  $\alpha$ -HH prepared by DH-S has the most intact hexagon-prism-sharped structure and the largest particle size among the three types of synthesized  $\alpha$ -HH. Cement-L presented the highest compressive strength. There was no obvious difference on the morphology of the three types of cements.

## Acknowledgements

The authors acknowledge the financial support from the Swedish Innovation Agency (VINNOVA) and China Scholarship Council (CSC).

## References

- [1] Guan, B., Yang, L., Fu, H., Kong, B., Li, T.Y. and Yang, L.C. (2011)  $\alpha$ -Calcium Sulfate Hemihydrate Preparation from FGD Gypsum in Recycling Mixed Salt Solutions. *Chemical Engineering Journal*, **174**, 296-303. <https://doi.org/10.1016/j.cej.2011.09.033>
- [2] Ling, Y. and Demopoulos, G.P. (2005) Preparation of  $\alpha$ -Calcium Sulfate Hemihydrate by Reaction of Sulfuric Acid with Lime. *Industrial Engineering Chemistry Research*, **44**, 715-724. <https://doi.org/10.1021/ie049316w>
- [3] Mao, J., Jiang, G., Chen, Q. and Guan, B. (2014) Influences of Citric Acid on the Metastability of  $\alpha$ -Calcium Sulfate Hemihydrate in CaCl<sub>2</sub> Solution. *Colloids and Surfaces A: Physicochemical and Engineering Aspects*, **443**, 265-271. <https://doi.org/10.1016/j.colsurfa.2013.11.023>
- [4] Guan, B., Shen, Z., Wu, Z., Yang, L. and Ma, X. (2008) Effect of pH on the Preparation of  $\alpha$ -Calcium Sulfate Hemihydrate from FGD Gypsum with the Hydrothermal Method. *Journal of American Ceramic Society*, **91**, 3835-3840. <https://doi.org/10.1111/j.1551-2916.2008.02729.x>
- [5] Singh, N.B. and Middendorf, B. (2007) Calcium Sulphate Hemihydrate Hydration Leading to Gypsum Crystallization. *Progress in Crystal Growth and Characterization of Materials*, **53**, 57-77. <https://doi.org/10.1016/j.pcrysgrow.2007.01.002>
- [6] Yang, L., Wu, Z., Guan, B., Fu, H. and Ye, Q. (2009) Growth Rate of  $\alpha$ -Calcium Sulfate Hemihydrate in K-Ca-Mg-Cl-H<sub>2</sub>O Systems at Elevated Temperature. *Journal of Crystal Growth*, **311**, 4518-4524. <https://doi.org/10.1016/j.jcrysgro.2009.08.013>
- [7] Jiang, G., Mao, J., Fu, H., Zhou, X. and Guan, B. (2013) Insight into Metastable Lifetime of  $\alpha$ -Calcium Sulfate Hemihydrate in CaCl<sub>2</sub> Solution. *Journal of American Ceramic Society*, **96**, 3265-3271.
- [8] Ishikawa, K. (2010) Bone Substitute Fabrication Based on Dissolution-Precipitation Reactions. *Materials*, **3**, 1138-1155. <https://doi.org/10.3390/ma3021138>
- [9] Rauschmann, M.A., Wichelhaus, T.A., Stiral, V., Dingeldein, E., Zichner, L., Schnettler, R. and Alt, V. (2005) Nanocrystalline Hydroxyapatite and Calcium Sulphate as Biodegradable Composite Carrier Material for Local Delivery of Antibiotics in Bone Infections. *Biomaterials*, **26**, 2677-2684. <https://doi.org/10.1016/j.biomaterials.2004.06.045>
- [10] Cooper, J.J. (2003) Method of Producing Surgical Grade Calcium Sulphate. United States Patent.
- [11] Cherdron, E., Pfalz, L., Forster, H.J. and Potencsik, I. (1973) Method of Precipitating Radium to Yield High Purity Calcium Sulfate from Phosphate Ores. United States Patent.

Appl. No. 350476.

- [12] Yang, J.C., Wu, H.D., Teng, N.C. and Lee, S.Y. (2014) Process for Preparing Alpha Calcium Sulfate Hemihydrate. United States Patent.
- [13] Feldmann, T. and Demopoulos, G.P. (2012) The Crystal Growth Kinetics of Alpha Calcium Sulfate Hemihydrate in Concentrated  $\text{CaCl}_2$ -HCl Solutions. *Journal of Crystal Growth*, **351**, 9-18. <https://doi.org/10.1016/j.jcrysgro.2012.04.014>
- [14] Guan, B., Kong, B., Fu, H., Yu, J., Jiang, G. and Yang, L. (2012) Pilot Scale Preparation of  $\alpha$ -Calcium Sulfate Hemihydrate from FGD Gypsum in Ca-K-Mg Aqueous Solution under Atmospheric Pressure. *Fuel*, **98**, 48-54. <https://doi.org/10.1016/j.fuel.2012.03.032>
- [15] Guan, B., Yang, L., Wu, Z., Shen, Z., Ma, X. and Ye, Q. (2009) Preparation of  $\alpha$ -Calcium Sulfate Hemihydrate from FGD Gypsum in K, Mg-Containing Concentrated  $\text{CaCl}_2$  Solution under Mild Conditions. *Fuel*, **88**, 1286-1293. <https://doi.org/10.1016/j.fuel.2009.01.004>
- [16] Freyer, D. and Voigt, W. (2003) Crystallization and Phase Stability of  $\text{CaSO}_4$  and  $\text{CaSO}_4$ -Based Salts. *Monatshefte für Chemie/Chemical Monthly*, **134**, 693-719. <https://doi.org/10.1007/s00706-003-0590-3>
- [17] Shen, Z., Guan, B., Fu, H. and Yang, L. (2009) Effect of Potassium Sodium Tartrate and Sodium Citrate on the Preparation of  $\alpha$ -Calcium Sulfate Hemihydrate from Flue Gas Desulfurization Gypsum in a Concentrated Electrolyte Solution. *Journal of American Ceramic Society*, **92**, 2894-2899. <https://doi.org/10.1111/j.1551-2916.2009.03330.x>
- [18] Prisciandaro, M., Lancia, A. and Musmarra, D. (2001) Calcium Sulfate Dihydrate Nucleation in the Presence of Calcium and Sodium Chloride Salts. *Industrial & Engineering Chemistry Research*, **40**, 2335-2339. <https://doi.org/10.1021/ie000391q>
- [19] Fu, H., Jiang, G., Wang, H., Wu, Z. and Guan, B. (2013) Solution-Mediated Transformation Kinetics of Calcium Sulfate Dihydrate to  $\alpha$ -Calcium Sulfate Hemihydrate in  $\text{CaCl}_2$  Solutions at Elevated Temperature. *Industrial & Engineering Chemistry Research*, **52**, 17134-17139. <https://doi.org/10.1021/ie402716d>
- [20] Yang, L., Guan, B., Wu, Z. and Ma, X. (2009) Solubility and Phase Transitions of Calcium Sulfate in KCl Solutions between 85°C and 100°C. *Industrial & Engineering Chemistry Research*, **48**, 7773-7779. <https://doi.org/10.1021/ie900372j>
- [21] Dirksen, J.A. and Ring, T.A. (1991) Fundamentals of Crystallization: Kinetic Effects on Particle Size Distributions and Morphology. *Chemical Engineering Science*, **46**, 2389-2427. [https://doi.org/10.1016/0009-2509\(91\)80035-W](https://doi.org/10.1016/0009-2509(91)80035-W)
- [22] Barlow, D.A., Baird, J.K. and Su, C.H. (2004) Theory of the Von Weimarn Rules Governing the Average Size of Crystals Precipitated from a Supersaturated Solution. *Journal of Crystal Growth*, **264**, 417-423. <https://doi.org/10.1016/j.jcrysgro.2003.12.047>
- [23] Fernandezdez, E., Vlad, M.D., Gel, M.M., Lopez, J., Torres, R., Cauich, J.V. and Bohner, M. (2005) Modulation of Porosity in Apatitic Cements by the Use of  $\alpha$ -Tricalcium Phosphate—Calcium Sulphate Dihydrate Mixtures. *Biomaterials*, **26**, 3395-3404. <https://doi.org/10.1016/j.biomaterials.2004.09.023>
- [24] Wang, P., Lee, E.J., Park, C.S., Yoon, B.H., Shin, D.S., Kim, H.E., Koh, Y.H. and Park, S.H. (2008) Calcium Sulfate Hemihydrate Powders with a Controlled Morphology for Use as Bone Cement. *Journal of American Ceramic Society*, **91**, 2039-2042. <https://doi.org/10.1111/j.1551-2916.2008.02358.x>

**Submit or recommend next manuscript to SCIRP and we will provide best service for you:**

Accepting pre-submission inquiries through Email, Facebook, LinkedIn, Twitter, etc.

A wide selection of journals (inclusive of 9 subjects, more than 200 journals)

Providing 24-hour high-quality service

User-friendly online submission system

Fair and swift peer-review system

Efficient typesetting and proofreading procedure

Display of the result of downloads and visits, as well as the number of cited articles

Maximum dissemination of your research work

Submit your manuscript at: <http://papersubmission.scirp.org/>

Or contact [jbnb@scirp.org](mailto:jbnb@scirp.org)